Different ophthalmologic findings in induced models of Holoprosencephaly in zebrafish

Johannes Bulk[1], Valentyn Kyrychenko[1] and Stephan Heermann[1,2]

[1] Department of Molecular Embryology, Institute of Anatomy and Cell Biology, Faculty of Medicine, University Freiburg, 79104 Freiburg, Germany
[2] Faculty of Health, Security, Society, Furtwangen University, Furtwangen, Germany

Corresponding author: stephan.heermann@hs-furtwangen.de

Abstract
Early forebrain development is a fascinating process and the fate of higher brain function but also the fate of visual perception largely depends on it. During gastrulation a single domain for the prospective telencephalon and a single eye field are localized in the anterior most region of the early neuroectoderm, the anterior neural plate (ANP). Importantly, these domains must be split as development proceeds, giving rise to two telencephalic lobes as well as to two optic vesicles, which are transformed into optic cups subsequently.
Holoprosencephaly (HPE) unfortunately is a rather frequent developmental disorder of the forebrain, during which the separation of the early precursor domains is hampered. Clinical manifestation can vary a lot, including the accompanying ophthalmologic findings.
Here we ask, whether anophthalmia is more severe than cyclopia, both being ophthalmologic findings in HPE. In this brief analysis, we make use of a recently established zebrafish model of HPE in which the early function of BMP antagonists is abrogated by the excessive induction of a BMP ligand. An early induction was resulting in retinal progenitors being stuck in the forebrain with no eye being formed. We attenuated the induction protocol to investigate whether the anophthalmia phenotype could be changed into a cyclopic phenotype. We found synophthalmia and ocular hypotelorism, however, not cyclopia. Based on this we propose that anophthalmia and cyclopia are both the strongest ophthalmologic finding, however, depending on the type of HPE underlying.

Key words: holoprosencephaly, crypt-oculoid, BMP, *bmp4*, anophthalmia, cyclopia

Introduction

Holoprosencephaly (HPE) is a quite frequent pathology during early forebrain development (Matsunaga and Shiota, 1977) in which the splitting of precursor domains of the Anterior Neural Plate (ANP) is hampered. HPE is mostly caused by genetic defects, however, also environmental risk factors/ triggers are described (Addissie et al., 2021; Roessler et al., 2018). Both, the presumptive telencephalic lobes as well as both retinae are derivatives of the ANP. Thus, it is consistent that ophthalmologic phenotypes are associated with HPE (Pineda-Alvarez et al., 2011). Ophthalmologic phenotypes are e.g. ocular hypotelorism of different grades of severity with its strongest form being a single eye located at the center of the head, termed cyclopia. However, e.g. also coloboma and anophthalmia can be associated, although not all forms of anophthalmia can be considered part of the HPE spectrum (Fallet-Bianco, 2018; Loosli et al., 2003; Pineda-Alvarez et al., 2011).
We found that bmp antagonism is crucial for various consecutive steps of eye development ranging from splitting of the ANP, out-pocketing of optic vesicles, transformation from optic vesicle to optic cup and formation of the optic fissure and fusion of the optic fissure (Bulk et al., 2023; Eckert et al., 2019; Heermann et al., 2015; Knickmeyer et al., 2018). Our findings suggest a smooth transition of these processes, all being crucially affected by BMP signaling.
The smooth transition of theses developmental processes further explains, why so many different ophthalmologic phenotypes are possible in association with HPE and noticeably, why also coloboma can be found associated with HPE.

Using the zebrafish as a model system, we previously described two experimentally induced forms of HPE presenting different ocular phenotypes. In both of these two forms BMP signaling was affected. In the first form an experimental induction of *bmp4*, oversaturating endogenous BMP antagonists, resulted in anophthalmia, regularly. Here, retinal precursors were found stuck in a dysmorphic forebrain, termed “crypt-oculoid” (Bulk et al., 2023).
In the second form, based on the acute targeted inactivation of *bmp7b* and *bmpr1ba* respectively, various ophthalmologic phenotypes were observed. These phenotypes were ocular hypotelorism of various degree, synophthalmia and even cyclopia and cases of anophthalmia. These phenotypes can in principle be understood as different levels of severity, likely found due to the experimental setup of an acute intervention and analysis in the F0 generation. The phenotypes are all reflecting a disturbed division process of the ANP. Interestingly, only a few cases of anophthalmia were seen and these did not contain crypt-oculoids (Kyrychenko et al., in preparation).

Our previous findings suggest why a considerable mild ophthalmologic phenotype like coloboma can be found in HPE. We now wondered what the most severe ophthalmologic phenotype associated with HPE would be. Is it cyclopia or is it anophthalmia?

In this brief article we ask the following questions: “Is there an ocular phenotypic default in HPE? If so, is it Cyclopia or is it rather anophthalmia? Is anophthalmia more severe than cyclopia or is it just a different ophthalmic phenotype?”

Results

Anophthalmia or cyclopia?

We aimed to address our questions with the help of our first experimental model. We reasoned, that if anophthalmia is more severe than cyclopia, a less intense induction of

bmp4 might result in cases of cyclopia instead of anophthalmia. In order to address this, we performed milder induction paradigms of *bmp4* expression (**Figure 1, scheme of experimental design**). We now performed shorter heat shocks at 8.5 hpf. We induced *bmp4* expression not for 15 minutes but for 10 minutes and in addition even less, for 7.5 minutes. We found, in both shorter induction paradigms, milder forms of HPE showing ventral synophthalmia/ ocular hypotelorism, stronger in the 10 minutes paradigm **(Figure 1 B, C, D**) than in the 7.5 minutes paradigm (**Figure E, F, G, please see H, I as control**). Importantly, we did not find cyclopia in either paradigm. This indicates that the assumption of anophthalmia being more severe than cyclopia unlikely holds true, at least for our paradigm.

It rather suggests that synophthalmia and ocular hypotelorism are less severe forms of both cyclopia and anophthalmia and that the decision of whether a single cyclopic eye is formed is made on a different level.

Why no optic cup but rather a crypt-oculoid?

A strong and early induction of *bmp4* (15 min at 8.5 hpf) resulted in anophthalmia with crypt-oculoids (Bulk et al., 2023). An interaction between pre-lens ectoderm and optic vesicle is fundamental for the transformation of an optic vesicle into an optic cup (Hyer et al., 2003). A lens could not be identified in the respective embryos by gross morphological analysis. We next asked if nonetheless lens-like tissue could be detectable after a strong induction of *bmp4*. We thus addressed the expression of *cryaa* by wmish after such strong induction (**Figure 2 A, scheme**). *Cryaa* was found expressed in lenses of control embryos (**Figure B, C)**. It could also be detected in the induced embryos. Unexpectedly, we found it expressed anterior to the crypt-oculoid in *bmp4* induced embryos. Even though this is the region in which a lens would be formed in a cyclopic eye, a proper lens failed to form and importantly optic cup formation did not occur (**Figure D, E**).

Is the basal constriction of retinal progenitors affected by *bmp4* induction?

We next aimed to address why the retinal progenitors failed to form an optic cup in the strong *bmp4* induction paradigm (15 min at 8.5 hpf) which was resulting in crypt-oculoids (Bulk et al., 2023). During normal eye morphogenesis, individual retinal progenitors undergo a change of shape turning them from a columnar shape into a wedge shape. This is driven by basal constriction (Martinez-Morales et al., 2009a). To be able to address whether this change of shape is affected by *bmp4* induction, we delayed the *bmp4* induction slightly and induced at 10 hpf instead of 8.5 hpf (**Figure 3 A, scheme of adjusted experimental design**). This was giving the eye-field the necessary time to start dividing and the optic vesicles the necessary time to start out-pocketing (**Figure 3 B**). We used the transgenic line *tg(rx2:GFPcaax)* to visualize the retinal progenitors. We crossed this line to the *bmp4* inducible line and induced *bmp4* at 10.5 hpf for 15 minutes (**Figure 3 A scheme**). Notably, two vesicle like structures appeared on both sides (**Figure 3 B, B'**). The surface of the vesicles, however, remained flat and the shape changes of the retinal progenitors could not be observed as in controls (**Figure 3 B', close up of B, please see C and C' as control**). At 74 hpf the phenotype morphologically resembled the opo mutant phenotype (Martinez-Morales et al., 2009a) (**Figure 3 F,G, please see D, E as control**). These findings suggest that basal constriction is negatively affected by *bmp4*, induced at 10.5 hpf for 15 minutes, a late induction paradigm.

We then addressed the expression of *cryaa* in this late induction paradigm. Unexpectedly, we did not detect *cryaa* after *bmp4* was induced at 10.5 hpf for 15 minutes (**Figure J, K,**

please see H, I as control). It seems possible, that the absence of lens tissue and presumably also the absence of pre-lens ectoderm could have an effect on the failures in cup formation observed in this late induction paradigm.
It is thus not clear whether the hampered basal constriction, which likely is preventing optic cup formation in the delayed induction paradigm, is also preventing the crypt-oculoid from turning turn into at least one optic cup, a cyclops, in the early induction paradigm.

How is the shape change of the retinal progenitors hampered?
The shape change of the progenitors during optic cup morphogenesis is controlled by *opo/ofcc1* (Bogdanović et al., 2012; Martinez-Morales et al., 2009a). V*sx2* was later found as an upstream regulator of *ofcc1* (Gago-Rodrigues et al., 2015).
For the next steps of our analyses, we went back to the original, early treatment paradigm of *bmp4* induction at 8.5 hpf for 15 minutes (Figure 4 A, scheme). We addressed whether the expression of *ofcc1* and *vsx2* is affected by induction of *bmp4*. In controls *ofcc1* can be found among many other domains in the optic cup. Expression could also be found in the region of the crypt-oculoid after induction of *bmp4* (**Figure 4 D, E, please see B, D as control**). Analysis of *vsx2* expression showed expression more specifically in the optic cup in controls (**Figure 4 F, G**) and expression in the crypt-oculoid in *bmp4* induced embryos (**Figure 4 H, I**).
These findings suggest that the process of basal constriction of the retinal progenitors is more likely affected by other means than by the level of *ofcc1* and *vsx2*.
The transcription factor *lhx2* was also found essential for the transformation of the optic vesicle into the optic cup (Porter et al., 1997). We thus also addressed its expression.
Also, the expression of *lhx2* could be detected in the crypt-oculoid after *bmp4* induction (**Figure 4 L, M**), while in controls at this stage it was found in telencephalon, diencephalon and ventral optic cup (**Figure 4 J, K**). This suggests that it is not likely the key to the failure in optic cup formation after *bmp4* induction.

Summary, Discussion and Conclusion
HPE is the most frequent developmental forebrain pathology in humans and the grade of severity also of the ophthalmological phenotypes accompanying HPE is manifold. We have recently provided two novel models for inducible HPE, both based on alterations of BMP signaling and both showing ophthalmologic phenotypes (Bulk et al., 2023)(Kyrychenko et al in preparation). In this present analysis we aimed to investigate what the most intense ophthalmologic phenotype associated with HPE is, cyclopia or anophthalmia.

Starting from the hypothesis that anophthalmia could be more severe than cyclopia we made use of the induction paradigm for *bmp4* and used milder forms of induction. Notably, we found forms of ocular hypotelorism and ventral synophthalmia, however, no cyclopia. This was suggesting that at least for this HPE model the most severe form was anophthalmia and the lesser severe forms being synophthalmia, but no cyclopia. We reasoned that the decision whether an eye is formed is made at a different level and does not merely reflect the severity of the phenotype.

We then addressed why no eye was formed in this specific HPE model. We found a central anterior expression domain of *cryaa* in the region where a cyclopic eye would have been formed, in embryos that underwent an early induction of *bmp4*. This might be interpreted as part of an anlage of a cyclopic eye. Nevertheless, such cyclopic eye was not formed in

consecutive stages of development in early induced embryos. Bearing in mind that retinal progenitors were found stuck in the dysmorphic forebrain, we wanted to investigate further, why they did not form an optic cup.

We next wanted to test whether the shapes of the retinal progenitor cells are able to change after induction of *bmp4*. This change of shape during normal development is an important motor for optic cup formation, driven by ojoplano (*opo*) (Martinez-Morales et al., 2009a). In order to be able to address this issue, we needed to slightly delay the induction of *bmp4*, giving the eye-field more time to start to out-pocket. This way, we were able to show that the delayed induction was impeding the shape changes. The resulting phenotype was resembling the *opo* mutant (Martinez-Morales et al., 2009b). To our surprise, however, we were not able to find *cryaa* expressing tissue in these embryos. This was indicating that the mechanism by which eye development was hampered in the delayed induction paradigm could be different.
It is, thus, still elusive by what exact mechanism the optic cup formation is prevented in the early *bmp4* induction paradigm. Addressing the expression of *opo*, its upstream regulator *vsx2* or *lhx2* was not giving further insights, as these factors were found expressed in the dysmorphic forebrain regions of the anophthalmic embryos.
But even though we cannot be sure whether the impeded shape changes are functionally involved in the decision whether or not an eye is formed the anophthalmia phenotype of the early induction paradigm, we showed that shape changes are functionally connected to bmp antagonism, overall. Our data indicate that bmp antagonism is important to allow the changes of shape. This is fitting well to the data which previously connected the "rim involution" and function of *opo* during optic cup formation (Sidhaye and Norden, 2017) and our data showing that bmp antagonism is important for optic vesicle to optic cup formation, driven by a "bilateral neuroretinal flow" (Heermann et al., 2015).

At last, we briefly want to point out two differences in between our inducible HPE models. This might eventually add for better understanding the different ophthalmologic phenotypes accompanying HPE. **(Figure 5, summary and comparison between HPE model (Kyrychenko et al., in preparation and (Bulk et al., 2023)).**

The first difference is that in the *bmp4* inducible HPE model the telencephalic domain as well as the eye-field failed to divide (Bulk et al., 2023) while in the HPE model based on the acute targeting of *bmp7b* only the eye-field failed to divide. It will need further investigation to what extend this difference is potentially differentially affecting the architecture of the forebrain and subsequently the interaction of e.g. surface ectoderm and retinal progenitors.

The second difference is the expression of the early eye-field transcription factor *rx3*. In the *bmp4* induction model the expression of *rx3* is largely reduced while the level of expression was found largely normal in the second HPE model, based on acute targeting of *bmp7b*.

Overall, further analyses are needed to understand different types of HPE and the ophthalmologic phenotypes which go along.

Materials and Methods:

Zebrafish care

Adult zebrafish were kept in accordance with the local animal welfare law and with the permit from the "Regierungspräsidium Freiburg": 35-9185.64/1.1. Fish were housed in a recirculating system at 28°C in a 12h light/ 12h dark cycle.
The following transgenic lines were used: *tg(hsp70l:bmp4, myl7:eGFP)*(Knickmeyer et al., 2018) and *tg(Ola.Rx2:EGFP-CAAX,myl7:EGFP)*(Heermann et al., 2015). Zebrafish embryos were grown in petri dishes containing zebrafish medium, 0.3g/l sea salt in deionized water. Melanin-based pigmentation was inhibited, if needed for downstream applications. To this end embryos were incubated in 0.2 mM phenylthiourea.

Heat shock procedures

Application of a heat-shock was used for heat-shock inducible transgenes. Embryos at different developmental stages were incubated in 1.5 ml reaction tubes at 37°C (heating block, Eppendorf Thermomixer). Onset and duration of the heat shock is indicated in the respective experimental setup.

In situ hybridization

Whole-mount ISHs (wmishs) were performed as described previously (Bulk et al., 2023). These probes were used: *vsx2* (Eckert et al., 2020), *ofcc1* F: GATGCTGCCAAGCTCTACTGG; R: TTCATCCTCTCGTGTTGCTCAT, *lhx2b* F: ATGCCTTCAATCAGCGGG, R: TCAGAAGAGGCTGGTTAAGG, probes for *cryaa* were designed cloning free (Hua et al., 2018). Sequences are: *cryaa* F: CCAACACCCTTGGTTCAGAC, *cryaa* R: GTAACAGGGATGGTGCGATCT

Image Processing

Images were recorded via microscopy (Nikon, binocular) and images were subsequently edited for presentation using the software ImageJ (Fiji) (Schindelin et al., 2012) and Inkscape (Inkscape Project. (2020). *Inkscape*. Retrieved from https://inkscape.org).

Acknowledgements

We want to thank all members of the Heermann lab for insightful discussions. We want to express special gratitude to Ute Baur for great technical assistance. Furthermore, we want to thank Eleni Roussa and Klaus Unsicker for support of the Heermann lab. For support in regards to publication we want to thank the Open Access Publication Fund of the University of Freiburg.

References:

Addissie, Y. A., Troia, A., Wong, Z. C., Everson, J. L., Kozel, B. A., Muenke, M., Lipinski, R. J., Malecki, K. M. C. and Kruszka, P. (2021). Identifying environmental risk factors and gene–environment interactions in holoprosencephaly. *Birth Defects Research* 113, 63–76.

Bogdanović, O., Delfino-Machín, M., Nicolás-Pérez, M., Gavilán, M. P., Gago-Rodrigues, I., Fernández-Miñán, A., Lillo, C., Ríos, R. M., Wittbrodt, J. and Martínez-Morales, J. R. (2012). Numb/Numbl-Opo antagonism controls retinal epithelium morphogenesis by regulating integrin endocytosis. *Dev. Cell* 23, 782–795.

Bulk, J., Kyrychenko, V., Rensinghoff, P. M., Ghaderi Ardekani, Z. and Heermann, S. (2023). Holoprosencephaly with a Special Form of Anophthalmia Result from Experimental Induction of bmp4, Oversaturating BMP Antagonists in Zebrafish. *Int J Mol Sci* 24, 8052.

Eckert, P., Knickmeyer, M. D., Schütz, L., Wittbrodt, J. and Heermann, S. (2019). Morphogenesis and axis specification occur in parallel during optic cup and optic fissure formation, differentially modulated by BMP and Wnt. *Open Biol* 9, 180179.

Eckert, P., Knickmeyer, M. D. and Heermann, S. (2020). In Vivo Analysis of Optic Fissure Fusion in Zebrafish: Pioneer Cells, Basal Lamina, Hyaloid Vessels, and How Fissure Fusion is Affected by BMP. *Int J Mol Sci* 21, 2760.

Fallet-Bianco, C. (2018). Neuropathology of holoprosencephaly. *Am J Med Genet C Semin Med Genet* 178, 214–228.

Gago-Rodrigues, I., Fernández-Miñán, A., Letelier, J., Naranjo, S., Tena, J. J., Gómez-Skarmeta, J. L. and Martinez-Morales, J. R. (2015). Analysis of opo cis-regulatory landscape uncovers Vsx2 requirement in early eye morphogenesis. *Nat Commun* 6, 7054.

Heermann, S., Schütz, L., Lemke, S., Krieglstein, K. and Wittbrodt, J. (2015). Eye morphogenesis driven by epithelial flow into the optic cup facilitated by modulation of bone morphogenetic protein. *Elife* 4,.

Hua, R., Yu, S., Liu, M. and Li, H. (2018). A PCR-Based Method for RNA Probes and Applications in Neuroscience. *Frontiers in Neuroscience* 12,.

Hyer, J., Kuhlman, J., Afif, E. and Mikawa, T. (2003). Optic cup morphogenesis requires pre-lens ectoderm but not lens differentiation. *Dev. Biol.* 259, 351–363.

Knickmeyer, M. D., Mateo, J. L., Eckert, P., Roussa, E., Rahhal, B., Zuniga, A., Krieglstein, K., Wittbrodt, J. and Heermann, S. (2018). TGFβ-facilitated optic fissure fusion and the role of bone morphogenetic protein antagonism. *Open Biol* 8,.

Loosli, F., Staub, W., Finger-Baier, K. C., Ober, E. A., Verkade, H., Wittbrodt, J. and Baier, H. (2003). Loss of eyes in zebrafish caused by mutation of chokh/rx3. *EMBO Rep.* 4, 894–899.

Martinez-Morales, J. R., Rembold, M., Greger, K., Simpson, J. C., Brown, K. E., Quiring, R., Pepperkok, R., Martin-Bermudo, M. D., Himmelbauer, H. and Wittbrodt, J. (2009a). ojoplano-mediated basal constriction is essential for optic cup morphogenesis. *Development* 136, 2165–2175.

Martinez-Morales, J. R., Rembold, M., Greger, K., Simpson, J. C., Brown, K. E., Quiring, R., Pepperkok, R., Martin-Bermudo, M. D., Himmelbauer, H. and Wittbrodt, J. (2009b). ojoplano-mediated basal constriction is essential for optic cup morphogenesis. *Development* 136, 2165–2175.

Matsunaga, E. and Shiota, K. (1977). Holoprosencephaly in human embryos: epidemiologic studies of 150 cases. *Teratology* 16, 261–272.

Pineda-Alvarez, D. E., Solomon, B. D., Roessler, E., Balog, J. Z., Hadley, D. W., Zein, W. M., Hadsall, C. K., Brooks, B. P. and Muenke, M. (2011). A broad range of ophthalmologic anomalies is part of the holoprosencephaly spectrum. *Am J Med Genet A* 155A, 2713–2720.

Porter, F. D., Drago, J., Xu, Y., Cheema, S. S., Wassif, C., Huang, S. P., Lee, E., Grinberg, A., Massalas, J. S., Bodine, D., et al. (1997). Lhx2, a LIM homeobox gene, is required for eye, forebrain, and definitive erythrocyte development. *Development* 124, 2935–2944.

Roessler, E., Hu, P. and Muenke, M. (2018). Holoprosencephaly in the genomics era. *Am J Med Genet C Semin Med Genet* 178, 165–174.

Schindelin, J., Arganda-Carreras, I., Frise, E., Kaynig, V., Longair, M., Pietzsch, T., Preibisch, S., Rueden, C., Saalfeld, S., Schmid, B., et al. (2012). Fiji: an open-source platform for biological-image analysis. *Nature Methods* 9, 676–682.

Sidhaye, J. and Norden, C. (2017). Concerted action of neuroepithelial basal shrinkage and active epithelial migration ensures efficient optic cup morphogenesis. *Elife* 6,.

Figures and legends:

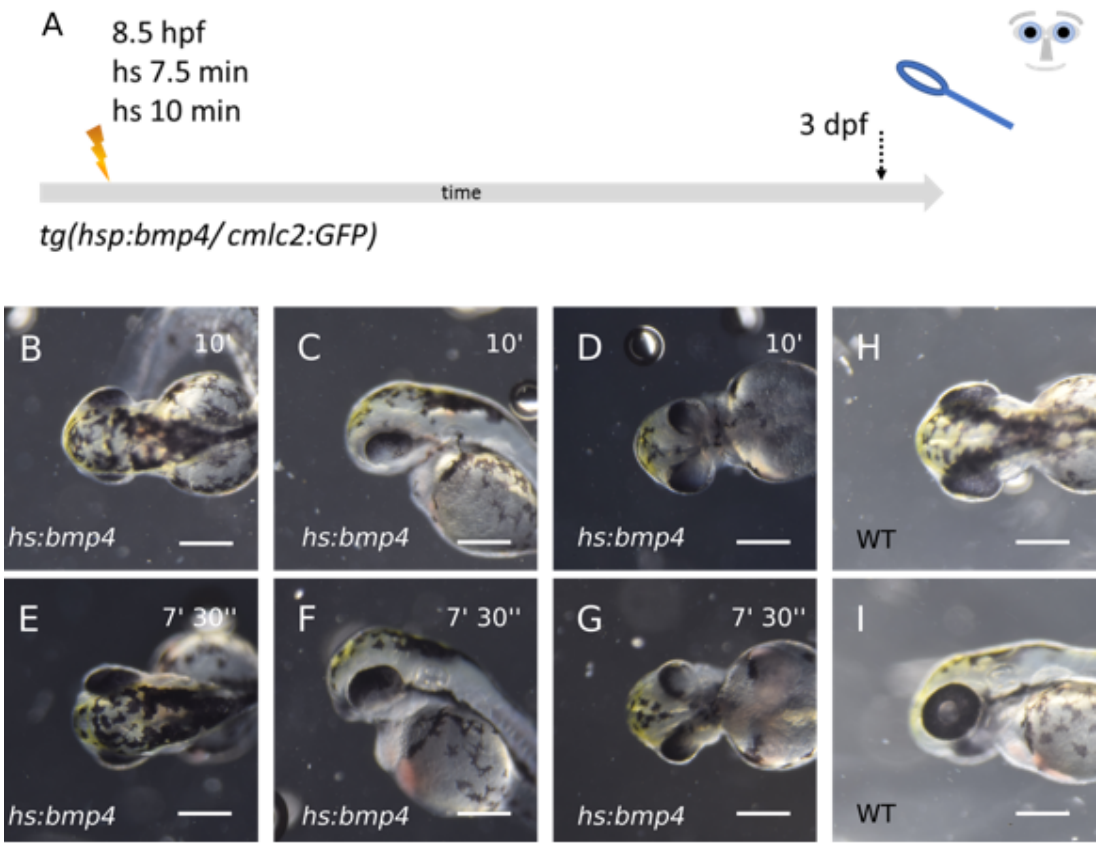

Figure 1

Figure 1, Inefficient bmp4-induction does not lead to cyclopia.
A: summary of experimental procedure: embryos were heat-shocked at 8,5 hpf for 7,5 or 10 min and analyzed 3 dpf. **B-D:** bmp4-induction for 10 min instead of 15 min. The fish develop two optic cups that are fused in the middle. **E-G:** bmp4-induction for 7,5 min. The fish develop a wide coloboma. H, I: Wildtypes at 3 dpf. **B, E, H:** dorsal views, **C, F, I:** lateral views, **D, G:** ventral views. Scalebars indicate 250 µm.

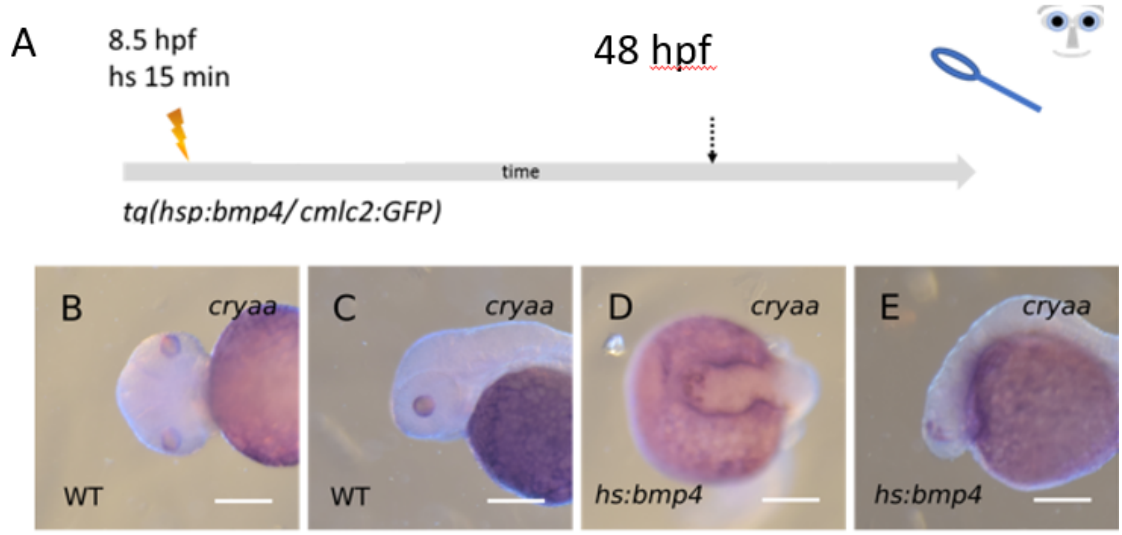

Figure 2

Figure 2, no eye but lens-like tissue in the anterior domain of the head
A: summary of experimental procedure: embryos were heat-shocked at 8,5 hpf for 15 min and analyzed at 48 hpf. **B-E:** ISH for *cryaa* at 48 hpf after a 15 min heat-shock at 8,5 hpf. **B, D:** dorsal views. **C, E:** lateral views. **B, C:** wildtype. **D, E:** *bmp4*-induction for 15 min at 8,5 hpf. The embryo has no eyes and multiple small *cryaa*-domains at the tip of the head. Scalebars indicate 200 µm.

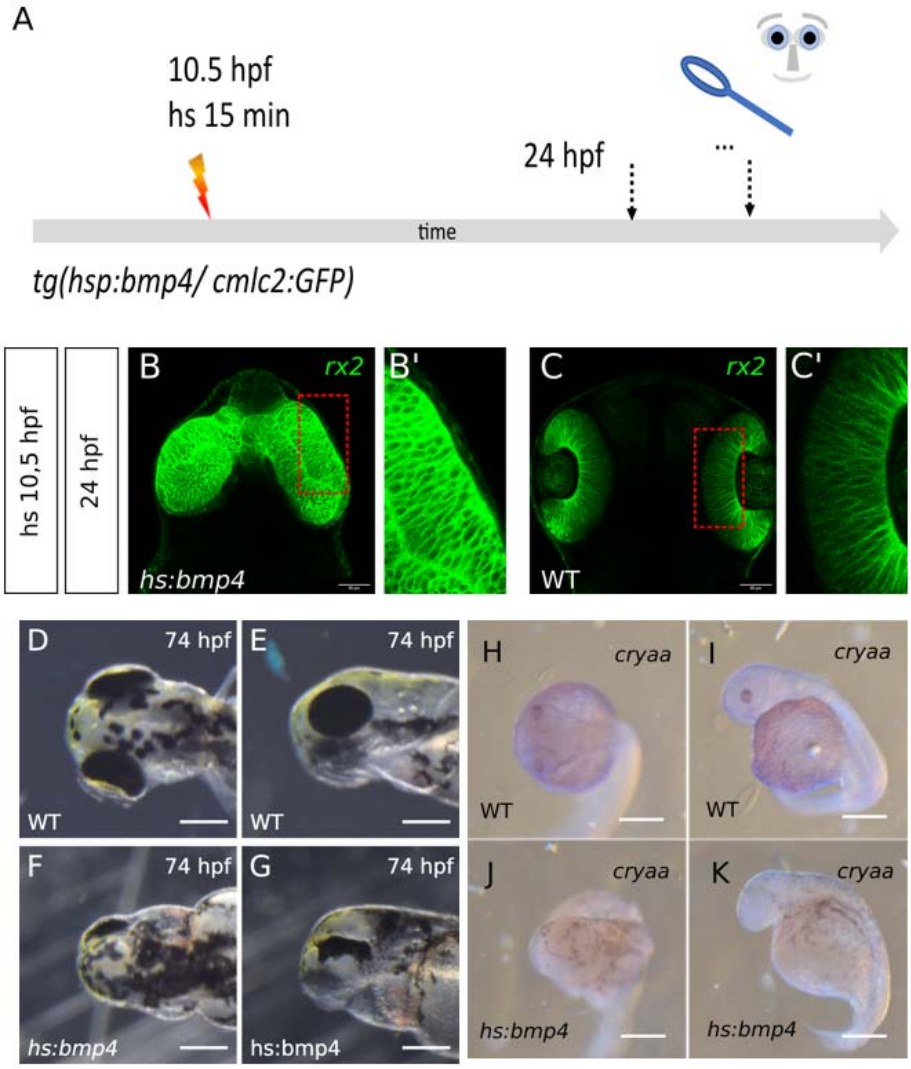

Figure 3

Figure 3, delayed *bmp4* induction results in "flat-eyes"
A: summary of experimental procedure: embryos were heat-shocked delayed at 10,5 hpf for 15 min and analyzed 24 hpf or at later stages. **B -C':** Confocal images with green indicating *rx2*-positive tissue at 24 hpf. **C, C':** wild-type. **B, B':** bmp4-induced at 10,5 hpf. Please note that the delayed induction resulted in out-pocketing of optic vesicles, which, however, were not transformed into optic cups. Scalebars indicate 50 µm. **C-G:** gross analysis at 74 hpf of embryos after a 15 min heat-shock at 10,5 hpf. **D, E:** wild-type. **F, G:** *bmp4*-induction for 15 min at 10,5 hpf. Please note that the induced embryos show a phenotype reminiscent of a flat-eye "ojoplano" phenotype (Martinez-Morales et al., 2009b). **D, F:** dorsal view. **E, G** lateral view. Scalebars indicate 250 µm**. H-K:** ISH for cryaa at 48 hpf after a 15 min heat-shock at 10,5 hpf. **H, I:** wild-type. **J, K:***bmp4*-induction for 15 min at 10,5 hpf. Please note that the embryo shows no eyes and no visible cryaa-positive tissue. **H, J:** dorsal view. **I, K:** lateral view. Scalebars indicate 250 µm**.**

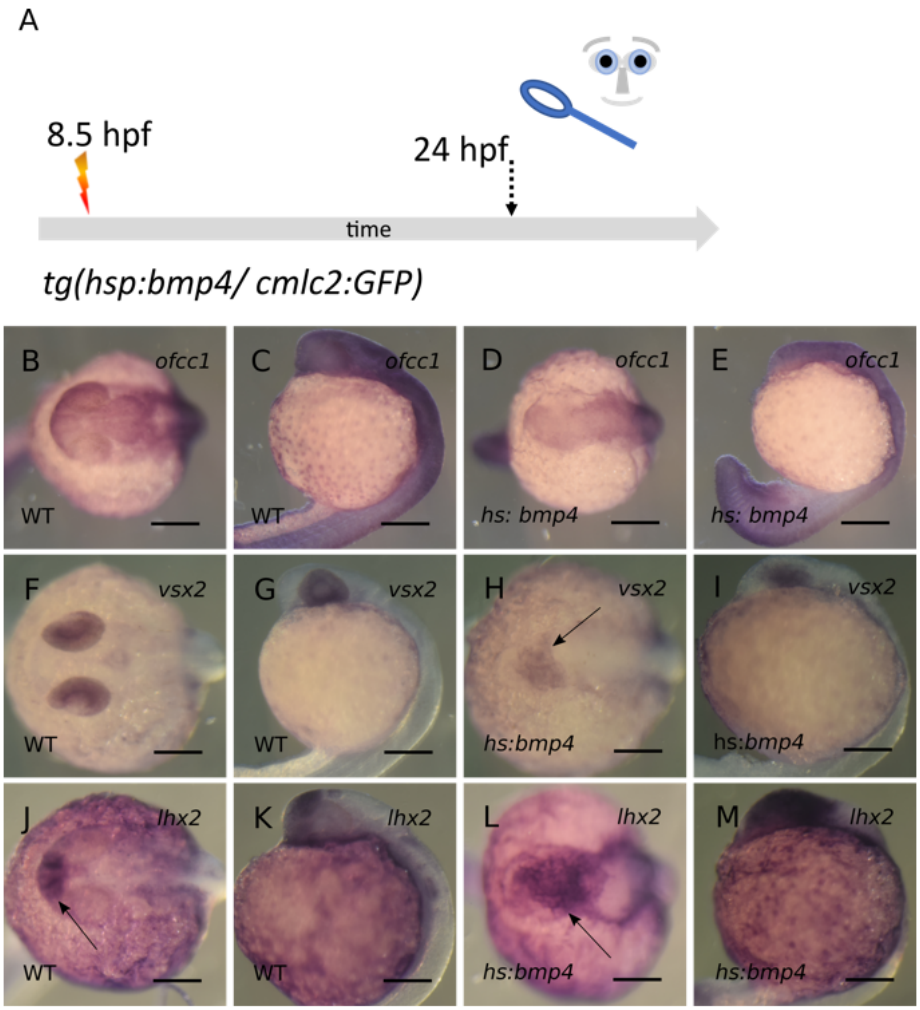

Figure 4

Figure 4

A: summary of experimental procedure: embryos were heat-shocked at 8,5 hpf for 15 min and analyzed 24 hpf. **B-M:** ISH at 24 hpf after 15 min heat-shock at 8,5 hpf. **B, C, F, G, J, K:** wildtypes, **D, E, H, I, L, M:** *bmp4* induced, **B, D, F, H, J, L:** dorsal view, **C, E, G, I, K, K:** lateral view, **B-E:** ISH for *ofcc1* (opo), *Ofcc1* expression persists after *bmp4* induction. **F-I:** ISH for *vsx2*, *vsx2* is expressed in the optic cup of wild-types and inthe crypt-oculoid (arrow). **J-M:** ISH for *lhx2*, *lhx2* is also expressed in the oculoid after bmp4 induction as well as in the telencephalon, diencephalon and ventral optic cup in wild-types (arrows). Scalebars indicate 200 µm.

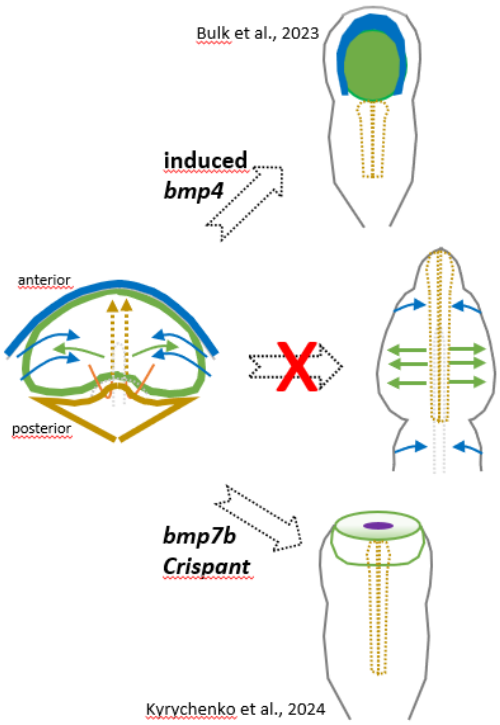

rx3	***cxcr4a***	***six3b***	***zic2a***	***rx2* in anophthalmia**
loss of expression	strongly reduced expression in the ANP	condensed expression at midline	loss of expression in the ANP	expression within „crypt-oculoid“
condensed expression close to midline	condensed expression close to midline	condensed expression close to midline	extended width between lateral expression domains, reduction of transverse domain in posterior ANP	loss of rx2 in anophthalmic embryos

Figure 5, comparison of HPE models

Figure 5, summary and comparison between HPE model (Kyrychenko et al., in preparation and (Bulk et al., 2023))